Dynamic Contrast-Enhanced MRI for Measuring Pancreatic Perfusion in Acute Pancreatitis: A Preliminary Study

Ran Hu, MS, Hua Yang, MD, Yong Chen, MS, Ting Zhou, MS, Ju Zhang, MS, Tian Wu Chen, MD, Xiao Ming Zhang, MD

Rationale and Objectives: To assess the characteristics of pancreatic perfusion in normal pancreas and acute pancreatitis (AP) by using dynamic contrast-enhanced (DCE) magnetic resonance imaging (MRI).

Method and Materials: Eighty-One AP patients and 26 normal subjects underwent DCE-MRI. The Omitk-Tool was used to analyze perfusion parameters such as K^{trans}, V_p, and AUC. The parameters of pancreas between AP and control groups were compared. In AP patients, the parameters were compared between edematous and necrotizing pancreatitis and among different grades of AP as determined by MR severity index (MRSI) and the 2012 Revised Atlanta Classification of AP.

Results: The K^{trans}, V_p, and AUC values of AP were lower than those of the control group ($p = 0.007$, 0.000, and 0.025). According to MRSI, the K^{trans} and AUC values were significantly different between mild and moderate ($p = 0.000$, 0.000) and between mild and severe ($p = 0.008$, 0.016) AP but not between moderate and severe AP ($p = 0.218$, 0.217). Based on the 2012 Revised Atlanta Classification, the K^{trans} values were significantly different between mild and moderately severe ($p = 0.000$) and between mild and severe ($p = 0.005$) AP, but not between moderately severe and severe AP ($p = 0.619$). The K^{trans} values were significantly different between edematous and necrotizing pancreatitis ($p = 0.03$).

Conclusion: The application of DCE-MRI to evaluate pancreatic perfusion contributes to the diagnosis of AP and its severity grade. Pancreatic perfusion is lower in AP patients than in patients with a normal pancreas, and pancreatic perfusion tends to decrease as the severity of AP increases.

Key Words: Pancreas; Acute pancreatitis; DCE-MRI.

INTRODUCTION

Acute pancreatitis (AP) is an inflammatory disease caused by autodigestion of the peripancreatic tissues and pancreatic parenchyma (1). Abnormal changes in the microcirculation can be found in AP, which make a significant difference to the early development and progression of AP (2). Previous studies have shown that perfusion CT can be used to determine the status of pancreatic perfusion to estimate AP severity at an early stage and to evaluate pancreatic ischemic damage to predict the progression of pancreatic necrosis in patients with early-stage AP (3–4). However, perfusion CT involves exposure to irradiation and requires intravenous injection of a potentially nephrotoxic iodinated medium. Moreover, it has been reported that the radiographic contrast medium, as used in contrast-enhanced CT, can reduce pancreatic perfusion and increase pancreatic necrosis in experimentally induced AP (5). And it has not been found the related reports on MRI contrast medium yet.

Recently, dynamic contrast-enhanced (DCE) magnetic resonance imaging (MRI) has emerged as a tool that can be used to assess the target tissue. DCE-MRI depends on acquiring a rapid sequence of images with high temporal resolution to analyze the relaxation effects of the contrast agent over the dynamic data-acquisition timeframe and to provide quantitative estimates of the physiological parameters associated with perfusion and/or permeability in vivo (6). Based on the pharmacokinetic model applied to fit the contrast-enhanced

Acad Radiol 2019; 26:1641–1649

From the Chongqing Traditional Chinese Medicine Hospital, Department of Radiology, No.6, Panxi 7th Road, Jiangbei District, Chongqing 400021, China (R.H., H.Y.); Sichuan Key Laboratory of Medical Imaging, Department of Radiology, Affiliated Hospital of North Sichuan Medical College, No.234, Fujiang Road, Shunqing District, Nanchong 637000, China (Y.C., T.Z., J.Z., T.W.C., X.M.Z.). Received January 18, 2019; revised February 11, 2019; accepted February 13, 2019. **Address correspondence to:** H.Y., X.M.Z. e-mails: 13527547568@163.com, cjr.zhxm@vip.163.com, Zhangxm@nsmc.edu.cn

https://doi.org/10.1016/j.acra.2019.02.007

curves, quantitative parameters can be derived that reflect the vascular and structural characteristics of the target tissue (7–8). Currently, DCE-MRI has been widely used in the diagnosis and therapeutic evaluation of pancreatic tumors. Nevertheless, the feasibility of DCE-MRI to evaluate pancreatic perfusion between AP and normal pancreas has not been investigated.

A number of scoring systems can be used to assess the severity of AP. There are two main categories: clinical assessment methods, including APACHE II score, Ranson's score and the 2012 Revised Atlanta Classification of AP; and radiological assessment methods, including the CT severity index (CTSI) and the MR severity index (MRSI) (9–12). Although the APACHE II scoring system reflects the severity of AP at admission, the scoring system is complex and mainly evaluates systemic complications without considering changes in the pancreas or evaluating organ failure (13). The Ranson's scoring system is usually calculated 48 hours after admission, which may delay treatment of the disease (9). Compared with the APACHE II score and Ranson's score, the 2012 Revised Atlanta Classification of AP is relatively simple and can evaluate the presence of organ failure as well as complications. In addition, according to the 2012 Revised Atlanta Classification of AP, the severity of AP can be graded as mild, moderately severe or severe, and acute pancreatitis includes edematous and necrotizing AP. Further, necrotizing AP can be classified as pancreatic parenchyma necrosis, peripancreatic tissue necrosis and combined necrosis, which contains pancreatic parenchyma and peripancreatic tissue necrosis. Among all the clinical evaluation methods, the 2012 Revised Atlanta Classification of AP provides clear definitions to classify AP using the identified radiologic and clinical assessments (12). CTSI is used to evaluate inflammation and pancreatic parenchyma necrosis in AP, and is considered the gold standard for assessing AP severity, pancreatic necrosis, local complications and clinical prognosis (14). It has been reported that MRSI is similar in quality to CTSI for assessing AP severity (15–16). Therefore, MRSI and the 2012 Revised Atlanta Classification of AP were selected as the criteria for AP severity grading in this study.

DCE-MRI has been used to evaluate the vascular and structural features of normal pancreas and pancreatic lesions (17–20). Akisik MF et al. applied DCE-MRI to assess antiangiogenic therapy in patients with locally-advanced pancreatic cancer (21). They established that DCE-MRI can characterize normal pancreatic microcirculation. However, the feasibility of DCE-MRI to evaluate pancreatic perfusion between an AP and a normal pancreas and the relationship between pancreatic perfusion parameters and AP severity has not been investigated. Therefore, we conducted this study using DCE-MRI to (1) measure the pancreatic perfusion parameters in patients with AP; (2) measure the pancreatic perfusion parameters in normal subjects; (3) compare the pancreatic perfusion parameters between AP and normal subjects; and (4) study the relationships in AP patients among the pancreatic perfusion parameters, MRSI and the Revised Atlanta Classification of AP in the early stages.

MATERIALS AND METHODS

Our institutional review board approved this study, and all participants signed the informed consent form.

Patients

AP patients who underwent DCE-MRI from September 2017 to December 2018 were recruited. The inclusion criteria were as follows: (1) typical acute abdominal pain; (2) the first occurrence of pancreatitis; (3) the level of serum amylase had increased to more than three times the normal value, excluding other causes of enzyme elevation; (4) upper abdominal DCE-MRI examinations within 14 days of the onset of AP; and (5) inpatient. We excluded 39 patients, including 15 for whom they could not hold breath during the coronal and axial SSFSE T2-weighted sequences and axial 3D LAVA-Flex sequence, or the patients were uncomfortable during the MRI examination so that they cannot complete the examination, 11 with chronic pancreatitis, 6 with pancreatic cancer, 4 for whom the examination was not performed within 14 days of the onset of pancreatitis, and 3 with liver disease. In total, 81 AP patients were enrolled in the AP group, including 46 men and 35 women, with a median age of 50.5 years (20–86 years).

Patients in the control group who underwent DCE-MRI were recruited from September 2017 to August 2018 from patients who underwent physical examinations for other disease assessments. The inclusion criteria were as follows: (1) no history of abdominal disorders; (2) sectional imaging showing a normal pancreas, with only liver cysts, hepatic hemangioma or renal cysts; and (3) no significant medical history of disease, including diabetes or other pancreatic disorders. We excluded 25 patients, including 9 with biliary diseases, 6 with cirrhosis, 6 with pancreatic diseases, and 4 with poor imaging results due to respiratory factors. Finally, 26 patients were enrolled in the control group, including 11 men and 15 women, with a median age of 46 years (20–67 years).

MRI Technique

DCE-MRI was performed within 14 days after the initial pancreatitis symptoms occurred. Patients were fasted for 6 to 8 hours before the DCE-MRI scan. A cummerbund was used to reduce respiratory motion artifacts. All DCE-MRI was performed with a 3.0 T MRI (US GE Discovery 750) in the supine position and equipped with a 32-channel phased-array surface coil.

The scanning sequences included axial fast-recovery fast spin-echo (FRFSE) T2-weighted imaging with fat suppression, two-dimensional coronal and axial single-shot fast spin-echo (SSFSE) T2-weighted imaging, an axial 3D LAVA-Flex

(axial three-dimensional liver acquisition with volume acceleration-flexible) sequence, and an axial 3D LAVA-Flex dynamic contrast-enhanced scan sequence.

Axial FRFSE T2-weighted images with fat suppression were obtained with the following parameters: TR, 10000-12000; TE,90-100; flip angle: 9°, thickness, 5 mm; matrix, 256 × 192; FOV, 36 × 34cm.

Coronal SSFSE T2-weighted images were obtained in two or more breath-holds. The parameters were following: TR, 2500-3500; TE,80-100; flip angle: 90°, thickness, 5 mm; matrix, 384 × 256; FOV, 39 × 33cm.

Axial SSFSE T2-weighted images were obtained in two or more breath-holds. The parameters were following: TR, 2500-3500; TE,80-100; flip angle: 90°, thickness, 5 mm; matrix, 320 × 256; FOV, 39 × 33cm.

Axial 3D LAVA-Flex MR images were obtained in one breath hold. The parameters used were following: repetition time (TR), 3.3; echo time (TE):1.5; flip angle: 3°, 6°, 9°, 12° and 15°(imaged five times with varying flip angles before the contrast material was injected); thickness, 6 mm; matrix, 360 × 280; field of view (FOV), 256 × 192cm.

Axial 3D LAVA-Flex dynamic contrast-enhanced scan sequence was obtained with the following parameters: TR,;3.3 TE, 1.5; flip angle: 15°, thickness, 6 mm; matrix, 360 × 280; FOV, 256 × 192cm, and the sequence continuously imaged for 304 seconds with the contrast material injected after imaging the third full-frame set.

Gadolinium chelate (Gadodiamide injection, General Electric Healthcare, Ireland) was administered intravenously (0.2 mmol/L per kg of body weight) at 2.5 mL/s using a double-tube high-pressure injector (Spectris MR Injection System, Medrad, Pittsburgh, PA) and was followed by a 20 mL saline solution flush at the same speed. All patients were instructed to breathe slowly during the examination.

Image Analysis

Three observers, having 5 to 6 years of experience interpreting pancreatic MR images, used a workstation (ICNRIS System) to review the original MR imaging data. They were blinded to the laboratory data and clinical outcomes.

The MRSI was derived from the CTSI (16), and the severity of AP was graded as mild (0−3 points), moderate (4−6 points), or severe (7−10 points) (Table 1).

According to the 2012 Revised Atlanta Classification of AP, the severity of AP was graded as mild, moderately severe and severe, which were respectively defined as no organ failure and no local or systemic complications; organ failure that resolves within 48 hours (transient organ failure) and/or local or systemic complications without persistent organ failure; and persistent organ failure (>48 h) including single or multiple organ failure (12).

DCE-MRI postprocessing software program (OmniKinetics Version V2.0.10, General Electric Healthcare) was used to generate the voxelwise perfusion maps of the volume transfer coefficient (K^{trans}), plasma volume (V_p) and area under the curve (AUC). First, T1 mapping was computed from the T1-weighted acquisitions with different flip angles ($\alpha = 3°$, 6°, 9°, 12° and 15). A region of interest (ROI) was manually drawn on the abdominal aorta to obtain an arterial input function (AIF). Three ROIs covering the pancreatic head, body, and tail were selected on the slice containing the maximum amount of pancreatic parenchyma. The area of each ROI was 20 mm^2 to 40 mm^2. The mean perfusion values of these ROIs were calculated and used. In necrotizing AP, a similar procedure was used to measure the perfusion parameters in the non-necrotic areas of the pancreas. That is, if the necrosis was in the head of the pancreas, the average of the perfusion parameters in the body and tail were used as the parameters of the whole pancreas. The visible vessels, pancreatic duct, necrotic areas, and cysts were not included in the ROIs.

TABLE 1. MR Severity Index Scoring System

Prognostic Indicator	Characteristic	Points
Inflammation	Normal pancreas	0
	Focal or diffuse enlargement of the pancreas	1
	Intrinsic pancreatic abnormalities with inflammatory changes in the peripancreatic fat	2
	Single, poorly defined fluid collection or phlegmon	3
	Two or more poorly defined collection or presence of gas in or adjacent to the pancreas	4
Necrosis	No necrosis	0
	<30%	2
	30%∼50%	4
	>50%	6

The K^{trans} depends on a balance between the capillary permeability and blood flow in the tissue of interest. In high-permeability situations, the K^{trans} mainly reflects the blood plasma flow per unit volume of tissue. In low-permeability situations, the K^{trans} mainly reflects the permeable surface area product between the blood plasma and the extravascular extracellular space (EES) per unit volume of tissue. V_p represents the total blood plasma volume. AUC mainly reflects the blood flow in the tissue of interest (8,22).

Statistical Analysis

Data were analyzed by using Statistical Package for Social Sciences (SPSS) for Windows (Version 13.0, Chicago, IL). Data derived from the MR images were averaged over the results of the three observers, and the perfusion values were averaged over multiple measurements. Any discrepancies would be

discussed by the three observers until a consensus was reached. The *chi-square* test was used to assess the interrater reliability of the MRSI and the 2012 Revised Atlanta Classification.

The median (interquartile) is used to present continuous variables. The number of cases or the percentage is used to present categorical data. The Wilcoxon signed-rank test was performed to compare the perfusion parameters among the head, body, and tail of normal pancreas. The *Wilcoxon* rank-sum test was performed to compare the perfusion parameters of the pancreas between the AP group and the control group, and the edematous and necrotizing AP group. The *Kruskal-Wallis H* rank-sum test was performed to compare the perfusion parameters of the pancreas among the different grades of AP as determined from MRSI and the 2012 Revised Atlanta Classification. The p values are 2-sided, and p values <0.05 were considered statistically significant.

RESULTS

Patient Sample

In the 81 patients with AP, the etiology of AP was biliary in 44.44% (36/81), alcoholic in 22.22% (18/81), hyperlipidemia in 17.28% (14/81), and unspecified in 16.05% (13/81) of the patients.

In the control group, the 26 total subjects included 15 subjects with no abnormalities, 5 subjects with hepatic cysts, 2 subjects with hepatic hemangiomas, and 4 subjects with renal cysts, according to their abdominal MRIs.

Perfusion Parameters of a Normal Pancreas

In the 26 subjects with a normal pancreas, the K^{trans}, V_p, and AUC values of the pancreas were (0.783, 0.416-1.073) mL/min, (0.299, 0.12-0.477), and (6.793, 5.486-9.397), respectively. The K^{trans} and AUC values of the normal pancreas were significantly different between the head and body ($p = 0.014$, 0.002) and between the head and tail ($p = 0.002$, 0.000), but not between the body and tail of the pancreas ($p = 0.17$, 0.253). The V_p values of the normal pancreas were not statistically significant among the different parts of the pancreas ($p = 0.431$, 0.082, and 0.298). Details regarding all p values are summarized in Table 2 and Figure 1.

Perfusion Parameters of a Pancreas with AP

In the 81 AP patients, the K^{trans}, V_p, AUC values of the pancreas were (0.505, 0.26−0.721) mL/min, (0.078, 0.037−0.201), and (5.256, 3.902−8.013), respectively. The inflammation of AP may be limited to the head, body or tail of the pancreas, thus the perfusion parameters in different parts of the pancreas with AP were not compared. The results are shown in Figures 2-4.

Comparison of the Perfusion Parameters Between AP and Normal Pancreas

The K^{trans}, V_p, and AUC values in AP patients were lower than those in patients with a normal pancreas, and these differences were statically significant (Z=−2.688, −3.763, and −2.237; and p = 0.007, 0.000, and 0.025, respectively).

Perfusion Parameters and the Grading Severity of AP According to MRSI

According to MRSI, the 81 patients with AP included 53.09% (43/81) with mild AP, 40.74% (33/81) with moderate AP, and 6.17% (5/81) with severe AP. The agreement among the three observers for the MRSI grading severity was very good ($X^2 = 1.436$, $p = 0.838$).

The K^{trans} and AUC values were significantly different between mild and moderate grades of AP (p = 0.000 and 0.000), and between mild and severe grades of AP ($p = 0.008$ and 0.016), but not between moderate and severe grades of AP (p = 0.218, and 0.271). However, the V_p value was not significantly different between the different severity grades of AP ($p = 0.444$, 0.161, and 0.252) (Table 3).

Perfusion Parameters and the Grading Severity of AP based on the 2012 Revised Atlanta Classification of AP

According to the 2012 Revised Atlanta Classification of AP, the 81 patients with AP included 41.98% (34/81) with mild AP, 53.09% (43/81) with moderately severe AP, and 4.94% (4/81) with severe AP. The agreement among the three observers for the 2012 Revised Atlanta Classification was very good ($X^2 = 1.256$, $p = 0.869$).

The K^{trans} value was significantly different between mild and moderately severe grades of AP ($p = 0.000$), and between

TABLE 2. Comparison of the DCE-MRI Perfusion Parameters in the Different Parts of the Pancreas (Median, Interquartile, $n = 26$)

	K^{trans} (mL/min)	V_p	AUC
Head	(0.92,0.478−1.424)	(0.349,0.098−0.47)	(9.599,5.553−12.927)
Body	(0.71, 0.405−0.992)	(0.22, 0.093−0.458)	(6.814, 4.361−8.594)
Tail	(0.652, 0.382−0.778)	(0.236, 0.064−0.435)	(5.257, 4.8−7.321)
Z value	−2.464*, 3.06**, 1.372***	−0.787*, 1.74**, -1.041***	−3.137*, 3.492**, 1.143***
p value	0.014*, 0.002**, 0.17***	0.431*, 0.082**, 0.298***	0.002*, 0.000**, 0.253***

Note: *represents head *vs.* body; **represents head *vs.* tail; ***represents body *vs.* tail.
AUC, area under the concentration curve; DCE-MRI, dynamic contrast-enhanced magnetic resonance imaging.

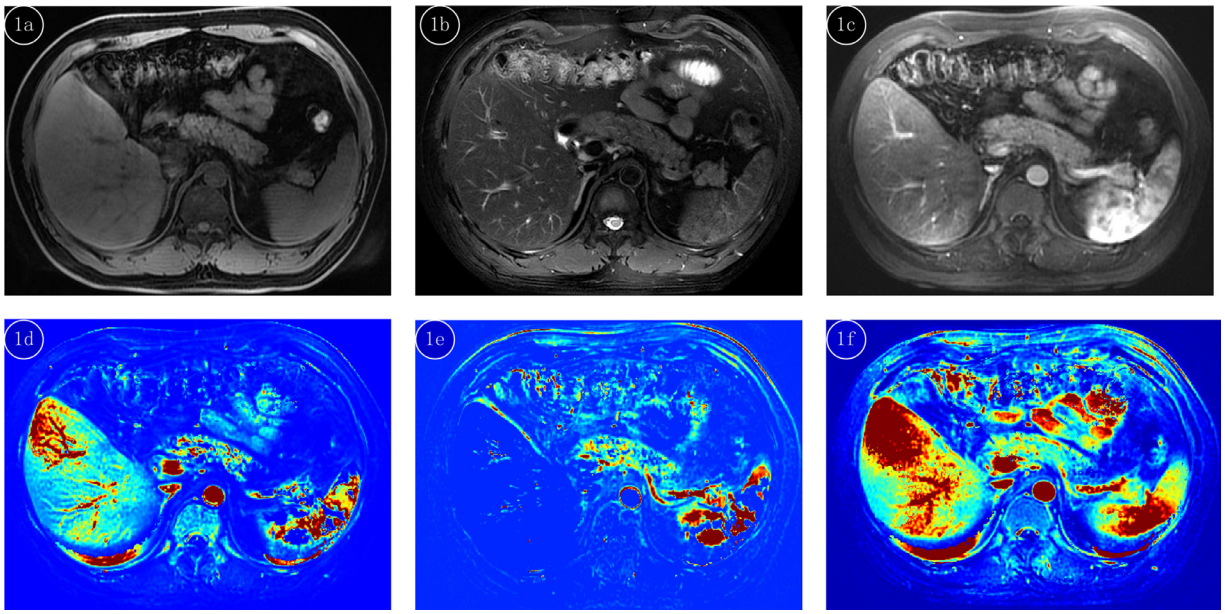

Figure 1. A 42-year-old male with a normal pancreas. **(a)** T1 WI; **(b)** Fat suppression T2 WI; **(c)** MRI-enhanced map; **(d)** K^{trans} map; **(e)** V_p map; and **(f)** AUC map. AP, acute pancreatitis; AUC, area under the concentration curve; MRI, magnetic resonance imaging.

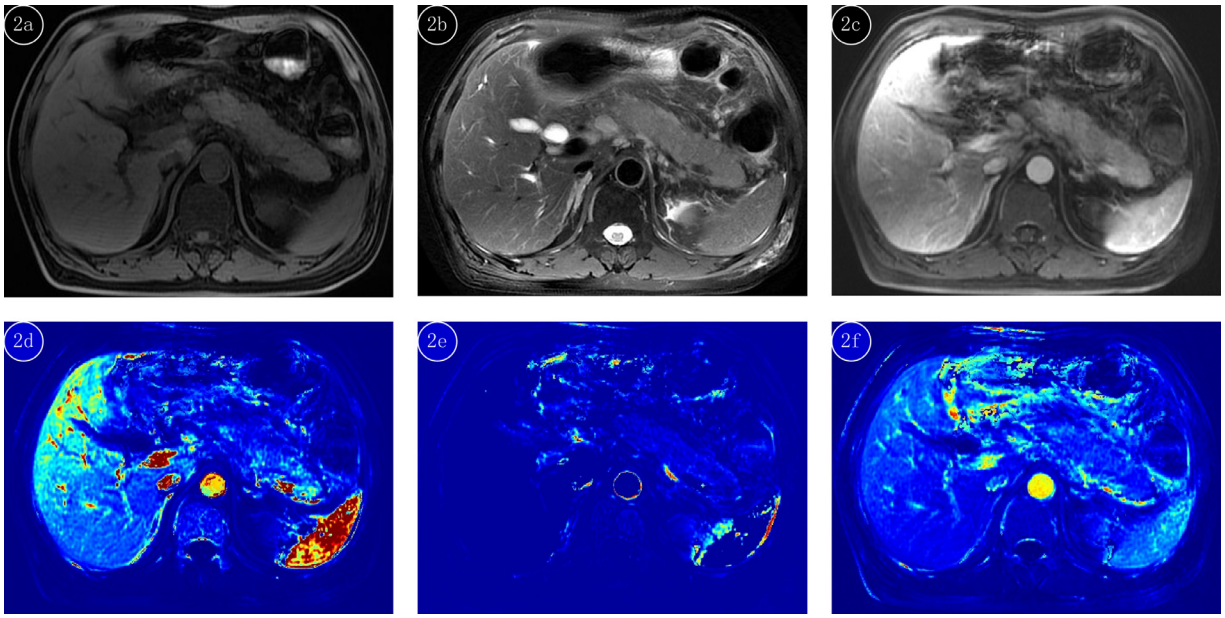

Figure 2. A 53-year-old male with edematous AP. The pancreas shows swelling and homogeneous enlargement **(a,c)**, and inflammatory exudation can be seen in the peripancreatic fat and the left renal anterior space **(b)**; **(d)** K^{trans} map; **(e)** V_p map; and **(f)** AUC map. AP, acute pancreatitis; AUC, area under the concentration curve.

mild and severe grades of AP ($p = 0.005$), but not between moderately severe, and severe grades of AP ($p = 0.619$) (Table 4).

Comparison of the Perfusion Parameters Between Edematous AP and Necrotizing AP

In the 81 patients with AP, 80.25% (65/81) and 19.75% (16/81) of the patients were classified as having edematous and necrotizing pancreatitis, respectively, based on MR images. In the 16 patients with acute necrotizing pancreatitis, 56.25% (9/16) and 43.75% (7/16) of the patients had peripancreatic tissue necrosis and combined necrosis, respectively.

The K^{trans} values between edematous and necrotizing AP were (0.598, 0.333−0.881) and (0.421, 0.241−0.51) mL/min, respectively, with a significant difference between the two groups ($Z = -2.171$, $p = 0.03$). However, the V_p and AUC values were not significantly different between edematous and necrotizing AP ($Z = -0.107$ and 0.937; and $p = 0.915$ and 0.349, respectively).

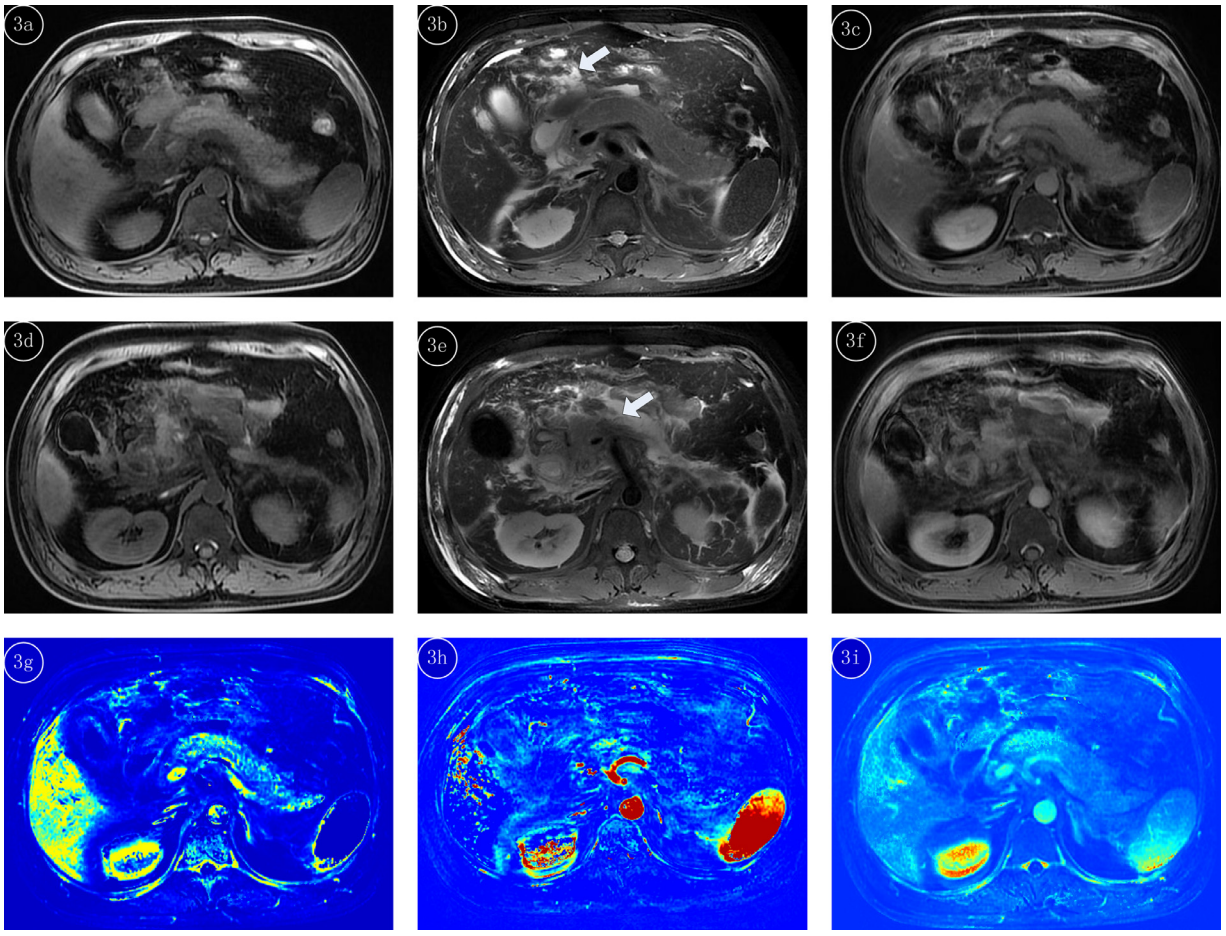

Figure 3. A 39-year-old male with peripancreatic tissue necrotic AP. T1 WI and the enhancement images show a swollen and homogeneously enlarged pancreas **(a,c)**. T1 WI, fat suppression T2 WI and the enhancement images show the nonliquid (arrows) and liquid peripancreatic components around the pancreas with no enhancement of the nonliquid peripancreatic components **(b, d-f)**. **(g)** K^{trans} map; **(h)** V_p map; and **(i)** AUC map. AP, acute pancreatitis; AUC, area under the concentration curve.

DISCUSSION

In this study, DCE-MRI can be applied to differentiate between an AP and a normal pancreas, and the K^{trans}, V_p and AUC values can be used as indicators to predict the severity of AP, which makes a significant difference in promoting timely treatment and improving patient prognosis.

In this study, the K^{trans} and AUC values in the head of normal pancreas were higher than those in the body and tail. The results were similar to those of previous studies applying DWI and gradient-echo T2∗-weighted imaging to research the ADC and T2∗ values in the different parts of normal pancreas (23−25). The difference in the values may be explained by the differences in the blood supply to the different parts of normal pancreas (26). Another potential explanation is the difference in tissue compositions between different parts of the pancreas. In other words, the number of Langerhans islets and the density of the fatty components are different between the pancreatic head, body and tail (25).

In this study, the K^{trans}, V_p and AUC values of AP were lower than those of normal pancreas. These results are similar to those of the CT perfusion parameters (blood flow and blood volume) used in a previous CT study, with the exception being that patients with AP showed higher permeable surface area products than did patients with normal pancreas (3). In this study, K^{trans} can reflect the capillary permeability, but K^{trans} depends on a balance between the capillary permeability and blood flow in the tissue of interest. In high-permeability situations, K^{trans} mainly reflects the blood plasma flow per unit volume of tissue (7). Investigators have reported that the capillary permeability of AP is high, with a tendency to increase with increasing severity of AP (27). In this case, the K^{trans} mainly reflects the blood flow in the target tissue, which is similar to the CT perfusion parameters (blood flow). During the development of AP, pancreatic acinar cells are the primarily affected cells, and inflammatory mediators are released into the pancreas, which can damage the endothelium and induce pancreatic microcirculation dysfunction, leading to poor pancreatic perfusion, pancreatic edema, and pancreatic necrosis (28−29). Therefore, our results clearly reveal the pathological characteristics of AP. Pancreatic

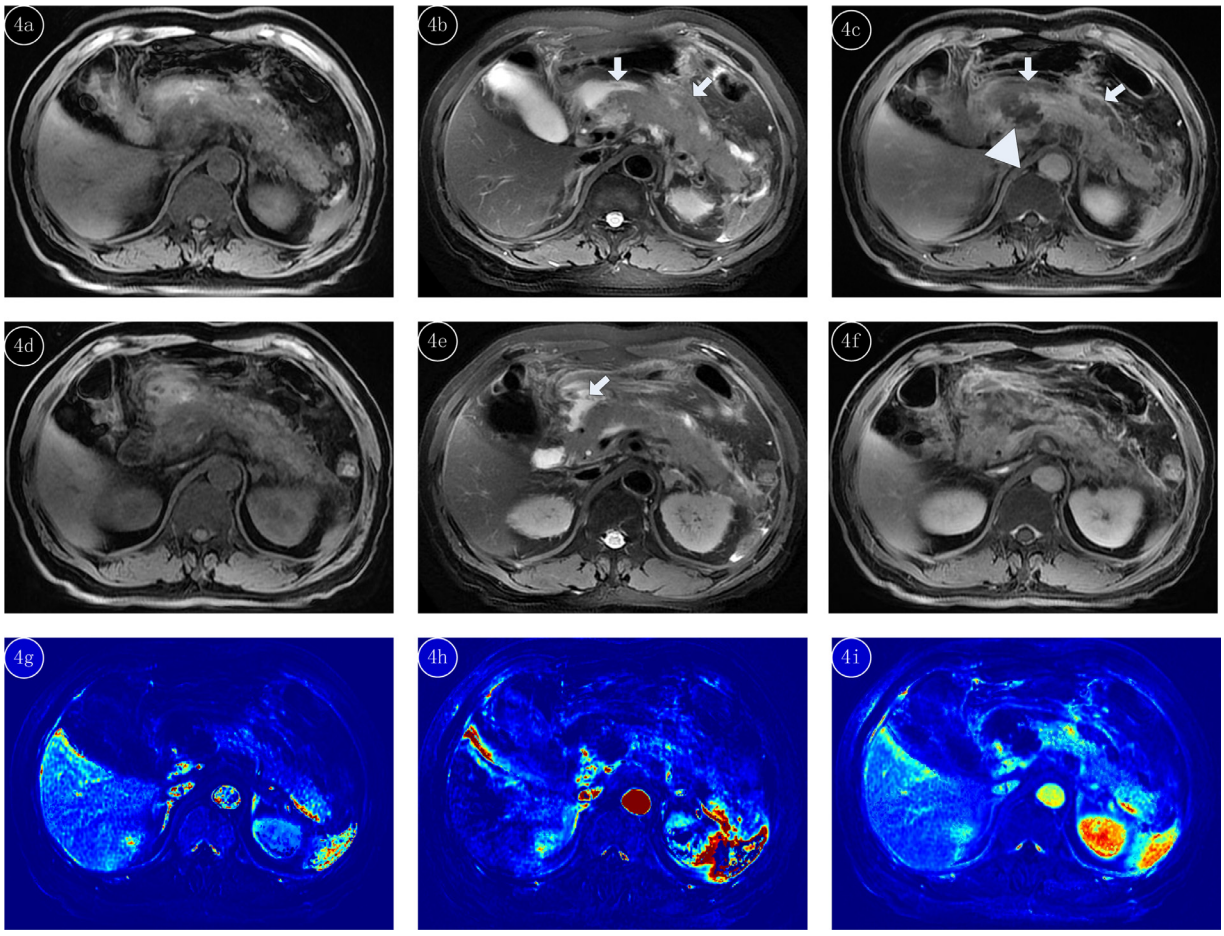

Figure 4. A 60-year-old male with combined necrotic AP. T1 WI, fat suppression T2 WI and the enhancement images show irregular necrosis in the pancreatic neck (triangle) and peripancreatic necrosis (arrows) **(a-f)**. **(g)** K^{trans} map; **(h)** V_p map; and **(i)** AUC map. AP, acute pancreatitis; AUC, area under the concentration curve.

perfusion in the AP patients is poorer than that in the control patients, and the K^{trans}, V_p and AUC values obtained by DCE-MRI can potentially be used as diagnostic indicators for AP.

MRSI originates from the CTSI developed by Balthazar, which mainly evaluates the inflammation and necrosis of the pancreas (14). In this study, the K^{trans} and AUC values decreased as the severity of AP increased based on MRSI, while the values between moderate and severe AP were not significantly different. K^{trans} and AUC mainly reflect the blood flow in the tissue of interest. A previous CT perfusion study has reported that pancreatic perfusion is worse in severe pancreatitis than in mild pancreatitis, according to Balthazar's criteria (30). In addition, investigators have reported that as the severity of MRSI increases, the conditions of AP patients become more serious (23,31). Therefore, we can speculate that the higher the severity of AP, the poorer the pancreatic perfusion, according to MRSI. The failure of pancreatic microcirculation can lead to acinar cell necrosis and edema level increases (32). Both the moderate and severe AP groups included patients with necrotizing AP, which may result in the K^{trans} and AUC values showing no statistically significant

TABLE 3. The Perfusion Parameters Among the Different Severities of AP Based on MRSI (Median, Interquartile)

Group	K^{trans} (mL/min)	V_p	AUC
Mild (n = 43)	(0.662, 0.417–0.833)	(0.092, 0.038–0.213)	(5.665, 4.599–8.432)
Moderate (n = 33)	(0.465, 0.158–0.56)	(0.089, 0.038–0.134)	(3.892, 3.094–5.961)
Severe (n = 5)	(0.18, 0.072–0.447)	(0.026, 0.022–0.155)	(3.302, 1.05–8.008)
Z value	-3.605^a, -2.649^b, 1.231^c	-0.765^a, 1.401^b, 1.145^c	-4.234^a, 2.413^b, 1.101^c
p value	0.000^a, 0.008^b, 0.218^c	0.444^a, 0.161^b, 0.252^c	0.000^a, 0.016^b, 0.271^c

Note: "a" represents mild *vs.* moderate; "b" represents mild *vs.* severe; "c" represents moderate *vs.* severe.
AUC, area under the concentration curve; AP, acute pancreatitis; MRSI, magnetic resonance severity index.

TABLE 4. The Perfusion Parameters of the Different Severities of AP Based on the 2012 Revised Atlanta Classification of AP (Median, Interquartile)

Group	K^{trans}(mL/min)	V_p	AUC
Mild ($n = 34$)	(0.712, 0.556−0.928)	(0.117, 0.036−0.209)	(6.134, 4.933−7.89)
Moderately severe ($n = 43$)	(0.381, 0.11−0.583)	(0.068, 0.042−0.135)	(4.453, 3.463−6.026)
Severe ($n = 4$)	(0.285, 0.129−0.437)	(0.05, 0.025−0.205)	(4.428, 3.417−6.901)
Z value	-4.524^a, 2.806^b, 0.534^c	-1.067^a, 0.785^b, 0.400^c	-3.18^a, 1.57^b, 0.152^c
p value	0.000^a, 0.005^b, 0.619^c	0.286^a, 0.432^b, 0.699^c	0.001^a, 0.116^b, 0.879^c

Note: "a" represents mild *vs.* moderately severe; "b" represents mild *vs.* severe; "c" represents moderately severe *vs.* severe.
AUC, area under the concentration curve; AP, acute pancreatitis.

difference between the moderate AP and severe AP groups. However, it is possible that the number of patients with severe AP was not large enough to attain a significant difference between the moderate and severe AP groups.

The 2012 Revised Atlanta Classification of AP has the advantage of reflecting the presence of organ failure and complications (12). In general, the higher the AP severity is, the more serious the general condition of the patient. In this study, the K^{trans} value was higher in mild AP than in moderately severe and severe AP. Mild AP was classified as having no organ failure or complications. Organ failure and complications can lead to increased morbidity and mortality in AP patients (33). Therefore, we speculate that pancreatic perfusion is higher in mild AP than in moderately severe and severe AP.

In the study, 16 AP patients had signs of necrosis, including peripancreatic tissue necrosis and combined necrosis, while 65 patients had acute edematous pancreatitis. The K^{trans} value in acute edematous pancreatitis was higher than that in acute necrotic pancreatitis. It has been reported that the severity of peripancreatic tissue necrotic AP is lower than that of combined necrotic AP, but it is higher than that of acute edematous pancreatitis (34−36). In addition, during the development of AP, failure in the microcirculation can lead to an increase in the level of acinar cell necrosis and edema (32). We can speculate that pancreatic perfusion is higher in edematous pancreatitis than in necrotic pancreatitis.

However, the sample size of the patients with severe AP was not large enough, which may have led to a slight bias in our results. A greater number of patients will be recruited in our future studies. The time interval between the DCE-MRI examination and the onset of AP was variable, which might have had an effect on the perfusion parameters and the grading severity of AP. We performed DCE-MRI examinations within 14 days of the onset of AP to minimize this variability.

In conclusion, the application of DCE-MRI to evaluate pancreatic perfusion contributes to AP diagnosis and severity grading. Pancreatic perfusion is significantly lower in AP patients than in patients with a normal pancreas, and pancreatic perfusion tends to decrease as the severity of AP increases.

REFERENCES

1. Forsmark ChE, Vege SS, Wilcox CM. Acute pancreatitis. N Engl Med 2017; 376:598–599.
2. Cuthbertson CM, Christophi C. Disturbances of the microcirculation in acute pancreatitis. Br J Surg 2006; 93:518–530.
3. Tian C, Xu X. Multislice spiral perfusion computed tomography to assess pancreatic vascularity in mild acute pancreatitis. J Comput Assist Tomogr 2017; 41:284–288.
4. Yadav AK, Sharma R, Kandasamy D, et al. Perfusion CT: Can it predict the development of pancreatic necrosis in early stage of severe acute pancreatitis. Abdom Imaging 2015; 40:488–499.
5. Schmidt J, Hotz HG, Foitzik T, et al. Intravenous contrast medium aggravates the impairment of pancreatic microcirculation in necrotizing pancreatitis in the rat. Ann Surg 1995; 221:257–264.
6. Oostendorp M, Post MJ, Backed WH. Vessel growth and function: depiction with contrast-enhanced MR imaging. Radiology 2009; 251:317–335.
7. Tofts PS. Modeling tracer kinetics in dynamic Gd-DTPA MR imaging. J Magn Reson Imaging 1997; 7:91–101.
8. Tofts PS, Brix G, Buckley DL, et al. Estimating kinetic parameters from dynamic contrast-enhanced T_1-weighted MRI of a diffusable tracer: standardized quantities and symbols. J Magn Reson Imaging 1999; 10:223–232.
9. Tang W, Zhang XM, Xiao B, et al. Magnetic resonance imaging versus acute physiology and chronic healthy evaluation II score in predicting the severity of acute pancreatitis. Eur J of Radiol 2011; 80:637–642.
10. Miller FH, Keppke AL, Dalal K, et al. MRI of pancreatitis and its complications: part 1, acute pancreatitis. AJR Am J Roentgenol 2004; 183:1637–1644.
11. Taylor SL, Morgan DL, Denson KD, et al. A comparison of the Ranson, Glasgow, and APACHE II scoring systems to a multiple organ system score in predicting patient outcome in pancreatitis. Am J Surg 2005; 189:219–222.
12. Banks PA, Bollen TL, Dervenis C, et al. Classification of acute pancreatitis−2012: revision of the Atlanta classification and definitions by international consensus. Gut 2013; 62:102–111.
13. Khan AA, Parekh D, Cho Y, et al. Improved prediction of outcome in patients with severe acute pancreatitis by the APACHE II score at 48 hours after hospital admission compared with the APACHE II score at admission. Acute physiology and chronic health evaluation. Arch Surg 2002; 137:1136–1140.
14. Balthazar EJ, Robinson DL, Megibow AJ, et al. Acute pancreatitis: value of CT in establishing prognosis. Radiology 1990; 174:331–336.
15. Stimac D, Miletić D, Radić M, et al. The role of nonenhanced magnetic resonance imaging in the early assessment of acute pancreatitis. Am J Gastroenterol 2007; 102:997–1004.
16. Lecesene R, Taourel P, Bret PM, et al. Acute pancreatitis: interobserver agreement and correlation of CT and MR cholangiopancreatography with outcome. Radiology 1999; 211:727–735.
17. Kim JH, Lee JM, Park JH, et al. Solid pancreatic lesions: characterization by using timing bolus dynamic contrast-enhanced MR imaging assessment—a preliminary study. Radiology 2013; 266:185–196.
18. Yao X, Zeng M, Wang H, et al. Evaluation of pancreatic cancer by multiple breath-hold dynamic contrast-enhanced magnetic resonance imaging at 3.0T. Eur J Radiol 2012; 81:e917–e922.

19. Kim H, Arnoletti PJ, Christein J, et al. Pancreatic adenocarcinoma: a pilot study of quantitative perfusion and diffusion-weighted breath-hold magnetic resonance imaging. Abdom Imaging 2014; 39:744–752.
20. Ma W, Li N, Zhao W, et al. Apparent diffusion coefficient and dynamic contrast-enhanced magnetic resonance imaging in pancreatic cancer: characteristics and correlation with histopathologic parameters. J Comput Assist Tomogr 2016; 40:709–716.
21. Akisik MF, Sandrasegaran K, Bu G, et al. Pancreatic cancer: utility of dynamic contrast-enhanced MR imaging in assessment of antiangiogenic therapy. Radiology 2010; 256:441–449.
22. Khalifa F, Soliman A, El-Baz A, et al. Models and methods for analyzing DCE-MRI: a review. Med Phys 2014; 41:124301.
23. Tang MY, Chen TW, Huang XH, et al. Acute pancreatitis with gradient echo T2*-weighted magnetic resonance imaging. Quant Imaging Med Surg 2016; 6:157–167.
24. Concia M, Sprinkart AM, Penner AH, et al. Diffusion-weighted magnetic resonance imaging of the pancreas: diagnostic benefit from an intravoxel incoherent motion model-baded 3 b-value analysis. Invest Radiol 2014; 49:93–100.
25. Schoennagel BP, Habermann CR, Roesch M, et al. Diffusion-weighted imaging of healthy pancreas: apparent diffusion coefficient values of the normal head, body, and tail calculated from different sets of b-values. J Magn Reson Imaging 2011; 34:861–865.
26. Collins JM, Silva AC, Hayman LA. Arterial anatomy of the pancreas. Part 3: segmented computed tomography-angiography mapping of perineuralinvasion. J Comput Assist Tomogr 2010; 34:961–965.
27. Chen HM, Sunamura M, Shibuya K, et al. Early microcirculatory derangement in mild and severe pancreatitis models in mice. Surg Today 2001; 31:634–642.
28. Klar E, Werner J. New pathophysiologic knowledge about acute pancreatitis. Chirurg 2000; 71:253–264.
29. Karne S, Gorelick FS. Etiopathogenesis of acute pancreatitis. Surg Clin North Am 1999; 79:699–710.
30. Bize PE, Platon A, Becker CD, et al. Perfusion measurement in acute pancreatitis using dynamic perfusion MDCT. AJR Am J Roentgenol 2006; 186:114–118.
31. Ji YF, Zhang XM, Li XH, et al. Gallbladder patterns in acute pancreatitis. Acad Radiol 2012; 19:571–578.
32. Yildirim AO, Ince M, Eyi YE, et al. The effects of glycyrrhizin on experimental acute pancreatitis in rats. Eur Rev Med Pharmacol Sci 2013; 17:2981–2987.
33. Weitz G, Woitalla J, Wellhoner P, et al. Comorbidity in acute pancreatitis relates to organ failure but not to local complications. Z Gastroenterol 2016; 54:226–230.
34. Wang M, Wei A, Guo Q, et al. Clinical outcomes of combined necrotizing pancreatitis versus extrapancreatic necrosis alone. Pancreatology 2016; 16:57–65.
35. Rana SS, Sharma V, Sharma RK, et al. Clinical significance of presence and extent of extrapancreatic necrosis in acute pancreatitis. J. Gastroenterol Hepatol 2015; 30:794–798.
36. Bakker OJ, van Santvoort H, Besselink MG, et al. Extrapancreatic necrosis without pancreatic parenchymal necrosis: a separate entity in necrotising pancreatitis? Gut 2013; 62:1475–1480.